

ARTICLE

Adverse Effects of Condenser Cooling Seawater Temperature, Fouling, and Salinity on the Output Power and Thermal Efficiency of BWR NNPs

Said M. A. Ibrahim* Ismail M. A. Aggour

Mechanical Engineering Department, Faculty of Engineering, Al-Azhar University, Cairo, Egypt

ARTICLE INFO

Article history

Received: 10 April 2022

Accepted: 6 May 2022

Published Online: 13 May 2022

Keywords:

BWR NPP

Thermal efficiency

Temperature

Fouling

Salinity

ABSTRACT

Increasing the thermal efficiency in newly designed power stations is a priority. Keeping the efficiency in existed plants close to the rated one is of paramount importance. This research contributes to investigating the adverse effects of changes in condenser seawater coolant characteristics, (temperature, fouling, and salinity), on the thermal performance of a Boiling Water Reactor Nuclear Power Plant (BWR) NPP. A mathematical model is developed to relate seawater cooling temperature, fouling, and salinity to output power and thermal efficiency. The model also explains the impact of the condenser performance on power and efficiency. The thermal efficiency of the considered BWR NPP is reduced by 2.26% for a combined extreme increases in the condenser cooling seawater temperature, fouling factor of seawater and treated boiler feed water, and salinity by 10 °C, 0.0002, 0.00001 m²K/W, and 100 g/kg, respectively. A rise in the condenser efficiency from 40% - 100% results in an increase in the output power by 7.049%, and the thermal efficiency increases by about 2.62%. Conclusions are useful for reactor's design.

1. Introduction

The ultimate goal of designers of power stations whether thermal or nuclear, from the thermodynamic point of view, is to attain the maximum possible thermal efficiency. For operators thereafter, the job is to maintain and run the station close to the rated efficiency. The low temperature sink is the heat rejected by the condenser, which is a crucial component of power stations. Its proper operation

according to the design data is of paramount importance for the station to operate efficiently. There is a desirability of having a high temperature internally and a low temperature in the external environment. This consideration gives rise to desirably siting power plants alongside cold water. Most power plants have higher efficiencies in winter than in summer.

A power plant is designed according to pre-determined design conditions for optimum efficiency. However, in

*Corresponding Author:

Said M. A. Ibrahim,

Mechanical Engineering Department, Faculty of Engineering, Al-Azhar University, Cairo, Egypt;

Email: prof.dr.said@hotmail.com

DOI: <https://doi.org/10.30564/jmmmr.v5i1.4617>

Copyright © 2022 by the author(s). Published by Bilingual Publishing Co. This is an open access article under the Creative Commons Attribution-NonCommercial 4.0 International (CC BY-NC 4.0) License. (<https://creativecommons.org/licenses/by-nc/4.0/>).

practice rated conditions cannot be maintained as the time goes by, because inlet conditions are not as per design data, hence the efficiency and output power drop. A steam plant and the second cycle of a nuclear plant are composed of many components; each is designed for optimum operation in order to satisfy the overall plant efficiency. The condenser is not the largest piece of equipment in the plant, but it is a key item in determining the plant efficiency.

Surface condensers are the types usually used in power plants. The condenser is necessarily a large piece of equipment because more than 60% of the thermal energy produced by a plant ends up as low enthalpy heat because of the thermodynamic limitation of the Rankine cycle. This reject heat is dissipated by the condenser to the environment. The heat transfer area in a power plant's surface condenser easily dwarfs any other heat exchanger in the plant. The lower heat sink temperature means higher Carnot cycle efficiency. The upper heat reservoir is limited by material considerations. Therefore, attaining the lowest possible condensing temperature in the heat sink of the Rankine cycle is a primary goal in surface condenser design. Since the saturation temperature and pressure of steam are proportionally related at low pressures, the objective of low condensing temperature necessitates a low condenser operating pressure. The condenser reduces the turbine exhaust pressure so as to increase the specific turbine output.

The steam power plant performance strongly depends on its low pressure end operating conditions, where the condenser is the key component to do this. The thermal efficiency of power plants mainly depends on its turbine-condenser performance. Generally, as the condenser pressure increases, due to changes in its cooling water characteristics, both thermal efficiency and net output power decrease and the steam consumption increases.

Condensers in power plants are usually cooled by water. Thus, factors affecting the condenser performance are related to characteristics of the condenser cooling water. The present research deals with nuclear power plants (NPPs), which are mostly located near seas, and condensers are cooled by seawater. Three properties of the condenser cooling seawater are important: temperature, fouling, and salinity. The adverse effects of these factors, due to deviations from design values, on the thermal performance of a BWR NPP are investigated. In fossil fuel power plants (PPs), some of the heat discharged is in the flue gases through the stack, whereas in a NPP virtually all the waste heat has to be dumped into the condenser cooling water. Thermal PP's have an intrinsic advantage which enables them to run their internal boilers at higher temperatures than those with finely engineered nuclear

fuel assemblies which must avoid damage for safety. This means that the efficiency of modern fossil fuelled plants is typically higher than that of nuclear plants. A nuclear or thermal plant running at 33% thermal efficiency, for instance will need to dump more heat than ones with 36% efficiency. Nuclear plants currently being built have about 34%-36% thermal efficiency, depending on the site (especially concerning water temperature). Older NPPs are often only 32%-33% efficient.

The water temperature in oceans, lakes, seas, and rivers differs significantly from one site to another. The seasonal variations of water temperature differ depending on the location. The design of the condenser in a power station depends on the inlet cooling water temperature. Therefore, the station should be sited carefully, according to the cooling water temperature of the source; low temperature sites with less seasonal variations are preferable if in hand. Sometimes it is unavoidable to locate the plant on a high temperature water source like in the Arabian Gulf region. As the temperature of the condenser cooling water changes, the condenser pressure is directly affected, and this reflects on the plant performance. Cooling water temperature increase means condenser pressure increase, and consequently plant efficiency decrease. It has been concluded that for a proposed PWR NPP, the output power and the thermal efficiency of the plant decrease by approximately 0.3929% and 0.16%, respectively, for 1 °C increase in the temperature of the condenser cooling seawater^[1]. It is shown that an increase in the inlet cooling seawater temperature of 15 °C reduces the efficiency and the output power by 2% and 6%, respectively, of the 1450 MW power cycle of the APR 1400 PWR NPP in the United Arab Emirates located on the Arabian Gulf^[2]. A study on the effect of cooling water temperature on the thermal efficiency of a PWR NPP, found that an increase of 1 °C of the coolant water results in a decrease of about 0.45% and 0.12% in the power output and thermal efficiency of the plant, respectively^[3]. For nuclear power plants, a rise in temperature of 1 °C reduces the nuclear power by about 0.5% through its effect on the thermal efficiency^[4]. For a 225 MW steam PP, every 1 °C increase in the condenser cooling seawater temperature, the output power of the plant decreased by about 0.171%, the condenser pressure increased by about 5.146%, and the plant efficiency decreased by approximately 0.168%^[5]. Reference^[6] investigated, by a thermodynamic model, the impact of flow rate, temperature and velocity of the cooling water on the heat transfer and condenser effectiveness, for a coal fired plant, and found that 1 °C increase in the inlet temperature of cooling water leads to deviation of the condenser pressure by 0.59 kPa, which reduces the cycle heat transfer rate

by 0.36% and the unit generation by 33 MW. An experimental work on the performance of a steam condenser in a 600 MW thermal PP depicted that the plant efficiency increased from 38.83% to 39.45% by reducing the condenser pressure to 65.21 bar^[7]. A research on the effect of the condenser^[8]. For an increase of 30 °C in the inlet cooling water temperature, the annual cash flow decreases by million 3.6 Dollars, and the electricity production cost is increased to 0.148 cent/kWh^[8]. A Rankine cycle model for the secondary cycle of a VVER 1200 NPP showed a decrease in the thermal efficiency from 37.44% to 33.65% due to an increase in the condenser pressure from 4 kPa - 15 kPa, which was attributed to increase in the condenser cooling temperature and atmospheric temperature^[9].

Fouling of heat exchangers may be defined as the accumulation of undesirable deposits on heat transfer surfaces. The fouled layer creates an additional resistance to heat transfer, and the contraction of the flow area, due to fouling, results in an increased flow velocity for a given volumetric flow rate. Furthermore, the deposit is usually hydro dynamically rough so that there is an increased resistance to the fluid flow across the deposited surface. In shell and tube steam condensers, the cooling water flow velocity is usually low, and this gives rise to more fouling accumulation in the tubes. Thus, the problems associated with condenser fouling will be more pronounced. Therefore, the consequences of fouling are, in general, a reduction in the exchanger efficiency and other associated operating problems including excessive pressure drop across the exchanger. This affects the plant thermal performance. In order to cope with the expected fouling, the heat exchanger should have an additional area over that required to give the same heat rate in the clean condition. A model for studying the effect of changes in the condenser cooling seawater fouling on the thermal efficiency and output power of a PWR NPP, indicated that an increase in the condenser cooling seawater fouling factor in the range 0.00015 m²K/W-0.00035 m²K/W had led to a decrease in the plant output power and thermal efficiency of 1.36% and 0.448%, respectively^[10]. The effect of the thermal resistance of fouling on the power output of a condensing turbine, after one year of operation, indicated that for old condensers the fouling resistance could reach 0.0007 m²K/W, and this reduced the turbine power output by up to 4.1%, whereas for new condensers, the power output drop did not exceed 1.5%^[11]. A model to predict the effect of fouling effect of fouling on the thermal performance of evaporative coolers and condensers showed that the maximum decrease in effectiveness due to fouling was 78% for condensers^[12]. Research published^[13] showed that undesirable design procedures and operation problems of heat

exchangers typically oversize them by 70%-80% of which 30%-50% is attributed to fouling. It has been stated that if the overall heat transfer coefficient for the fouled condition is ½ the coefficient for clean condition, then the heat transfer area is doubled, and that the choice of the fouling resistance is crucial not only for efficient operation of the heat exchanger and its operating cost, but also on its capital cost^[14]. A study on the impact of water fouling properties on the thermal and hydraulic parameters of the shell and tube heat exchanger tubes demonstrated that minor change in the fouling layer thickness has direct effect on the heat transfer compared to the pressure drop for the heat exchanger^[15]. A model has been provided to study the effect of fouling on the effectiveness and water outlet temperatures of cooling towers demonstrated about 0.6% decrease in effectiveness and about 1.2% increase in the water outlet temperature^[16]. Reference^[17] studied the bio fouling control of seawater to achieve efficient operation of a power station, and reported that it is important for power plant designers to choose the most suitable control method to combat bio fouling in practical, economical, and environmentally acceptable manners.

Salinity is the saltiness or the quantity of salt dissolved in water, which is called saline water. This is usually measured in g salt/kg seawater. Salinity is a thermodynamic state variable that, along with temperature and pressure, governs physical characteristics like the density and heat capacity of saline water. Thus, changes in the salinity of the condenser cooling seawater could affect its performance. Salinity in closed seas, like the Dead Sea is much higher than that in oceans and large area seas, rivers and lakes have very lower salinities in comparison. A model was provided to obtain the effect of salinity of the condenser cooling seawater of a PWR NPP on the thermo-physical properties of seawater on the thermal performance of the plant revealed that increasing the condenser cooling seawater salinity by 10 g/kg, 50 g/kg, and 100 g/kg resulted in losses in the thermal efficiency of the plant by 0.011%, 0.06%, and 0.14%, respectively with respective reductions in the output power for the same salinity values of 0.033%, 0.039%, and 0.044%^[18]. An investigation on the effect of changing the salt content on many properties of seawater, such as density, thermal expansion, temperature of maximum density, viscosity, speed of sound, vapor pressure, etc. gives that knowledge of the way these parameters change, as well as the processes that cause the changes, are essential for the design of systems that will effectively operate in the ocean^[19]. A model relating the condenser cooling seawater salinity and temperature and the thermal efficiency of a PWR NPP reported a loss of 0.2% in the efficiency, for temperature and salinity values

of 5 K, and 10000 ppm^[20]. Reference^[21] investigated the thermal performance of a seawater cooling tower experimentally and theoretically, and found that the air effectiveness decreased with increasing the seawater salinity, with a maximum decrease of 15% for a salinity of 85 g/kg. A work connected with injecting seawater into the nuclear reactors of the Fukushima disaster (Japan, 2011), in order to cool down fuel elements, illustrated that seawater affects the heat transfer due to changes in salinity and other physical properties of the coolant^[22].

We could not detect research work concerning the combined effect of temperature, fouling, and salinity of the condenser cooling seawater on the thermal performance of NPPs except that by Ibrahim et al.^[23]. This study focused on a proposed PWR NPP, and showed that a significant loss in the plant output power and thermal efficiency of up to 8.242% and 2.77%, respectively, can result from an increase in the condenser cooling seawater temperature from 15 °C-30 °C, fouling factor from 0.00015 m²K/W-0.00035 m²K/W, and salinity from 0 g/kg.-100 g/kg.

Since the efficiency of NPPs is lower than that of thermal PPs, therefore, it is important to mitigate or prevent if at all possible all factors that reduce their efficiency. To achieve this, relations between such factors and the thermal efficiency and output power of NPPs should be studied and analyzed. The current research contributes to the adverse effects of variations in the condenser inlet cooling seawater temperature, fouling, and salinity on the thermal efficiency and power output of a proposed BWR NPP. The paper includes the individual effects of these properties as well their combined impacts. We developed a model, based on thermodynamic and heat balance considerations, to calculate the required effects, and numerical solutions were performed by a computer program. The work is related to a BWR NPP, since there is no research conducted on this type of plant relevant to the subject of the current research.

2. The Selected BWR NPP

The present study is concerned with the complete cycle of a typical BWR NPP. An OKG's Oskarshamn 3 (O3) NPP is selected as a case study of such a plant. Oskarshamn is one of three active nuclear power plants in Sweden. The plant is located about 30 kilometers north of Oskarshamn, on the Baltic Sea coast. In 1985, Oskarshamn 3 was phased in online and reached its full power of 1050 MW. In 1989, the power of O3 was scaled up to a maximum of 1200 MW. In 2012, the power was further increased to 1450 MW, making O3 one of the largest BWRs in the world.

The plant consists typically of a BWR, reactor coolant pump, high-pressure steam turbine (HPST), three

low pressure steam turbines (LPST), moisture separator and reheater (MS/R), deaerator feed water heater, two high-pressure feed water heaters (HPFWH), and three low pressure feed water heaters (LPFWH), condenser, bypass valve (BPV) which is essential to keep the pressure inside the reactor at 70 bar to ensure good and stable moderation, and necessary pumps (feed water and condensate pumps). Figure 1 is a schematic diagram showing the main components of the proposed plant^[24].

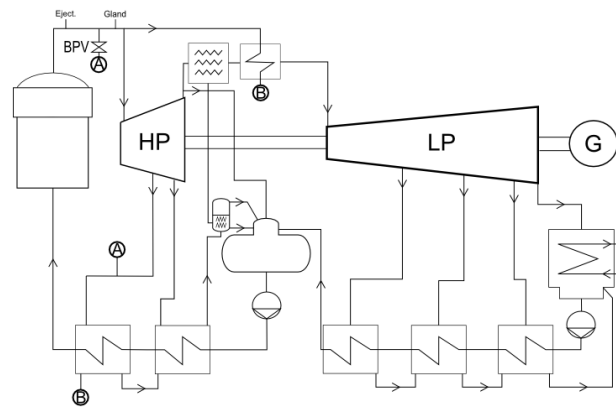


Figure 1. A Schematic of main components of the proposed BWR NPP

Technical design data of the Oskarshamn 3 NPP are given in Table 1.

Table 1. Design data of the Oskarshamn 3 BWR NPP

Vapor data		
before high pressure turbine	MPa / °C	6.5 / 283
after high pressure turbine	MPa / °C	0.97 / 179
in condenser	kPa / °C	4.0 / 30
Number of preheating steps		6
- low pressure preheating	stages	4
- high pressure preheating		2
Feed water temperature	°C	218
Generator power	MW	1450
Gross efficiency	%	36.5
Aggregate net power	MW	1400
Steam flow rate	Kg / s	2115
Condenser cooling water flow rate	m ³ / s	55
Condenser cooling water inlet temperature	°C	5
Condenser cooling water temperature increase	°C	10.5

3. The Present Theoretical Model

3.1 Model Calculation Data

The present calculations were made for these values:

- The range of change of cooling water temperature is 5 °C-15 °C.
- The range of change of the fouling factor, F is

0.00015 m²K/W-0.00035 m²K/W.

- The treated boiler feed water range is 0.00005 m²K/W-0.00015 m²K/W.
- The change of cooling seawater salinity S_p is 0 g/kg-100 g/kg.

The combined effect of cooling seawater temperature, fouling factor, and salinity was calculated for the above given values.

3.2 Model Assumptions

- (1) Thermodynamic conditions of the steam at exit of the nuclear reactor are fixed.
- (2) Thermal power of the BWR changes slowly to provide constant thermodynamic properties of the steam at exit from the nuclear reactor, since the variation in the cooling water temperature occurs seasonally and very slowly.
- (3) Constant cooling water temperature difference.
- (4) The condenser vacuum pressure varies with the temperature of cooling water extracted from the sea at fixed mass flow rate into the condenser.
- (5) Constant mass flow rates of condensate and cooling water.
- (6) Fixed total surface area of condenser tubes and material properties.
- (7) There is no pressure drop across the condenser.
- (8) Constant condenser heat transfer area and heat load.
- (9) Potential and kinetic energies of the flow and heat losses from all equipment and pipes are negligible.

3.3 Model Formulation and Equations

3.3.1 Thermodynamic Analysis

The energy balance equations for the various processes involving steady flow equipment such as the nuclear reactor, turbine, pumps, and condenser are:

♦ Heat added to steam from reactor, Q_{add} is

$$Q_{add} = \dot{m}_{st} (h_{out} - h_{in}) \text{ kW} \quad (1)$$

where \dot{m}_{st} = mass flow rate of steam exit from reactor or steam generator, kg/s, h_{in} = enthalpy of feed water inlet to reactor or steam generator, kJ/kg, and h_{out} = enthalpy of steam outlet from reactor or steam generator, kJ/kg.

♦ Total turbine work, W_T is

$$W_T = W_{HPT} + W_{LPT} \text{ kW} \quad (2)$$

$$W_{HPT} = \dot{m}_{st} (h_{in} - h_{out}) \text{ kW} \quad (3)$$

$$W_{LPT} = \dot{m}_{st} (h_{in} - h_{out}) \text{ kW} \quad (4)$$

where \dot{m}_{st} = mass flow rate of steam inlet to turbine, kg/s, h_{in} = enthalpy of steam inlet to turbine, kJ/kg, h_{out} = en-

thalpy of steam outlet from turbine, kJ/kg, W_{HPT} = high pressure turbine work, kW, and W_{LPT} = low pressure turbine work, kW.

♦ Pump work, W_p is

$$W_p = W_{cp} + W_{fwp} \text{ kW} \quad (5)$$

$$W_{fwp} = \dot{m}_{fw} (h_{in} - h_{out}) \text{ kW} \quad (6)$$

$$W_{cp} = \dot{m}_{fw} (h_{in} - h_{out}) \text{ kW} \quad (7)$$

where \dot{m}_{fw} = mass flow rate of feed water inlet to pump, kg/s, h_{in} = enthalpy of feed water to pump, kJ/kg, h_{out} = enthalpy of feed water outlet from pump, kJ/kg, W_{fwp} = feed water pump work, kW, and W_{cp} = condensate pump work, kW.

♦ Heat rejected from condenser, Q_{Rej} is

$$Q_{Rej} = (\dot{m}_{mix} * h_{in} - \dot{m}_{fw} * h_{out}) \text{ kW} \quad (8)$$

where \dot{m}_{mix} = mass flow rate of mixture inlet to condenser, kg/s, h_{in} = enthalpy of mixture inlet to condenser, kJ/kg, and h_{out} = enthalpy of feed water outlet from condenser, kJ/kg.

♦ Net work done, W_{net} is

$$W_{net} = W_T - W_p \text{ kW} \quad (9)$$

♦ Cycle efficiency, η_{th} is

$$\eta_{th} = \frac{W_{net}}{Q_{add}} \% \quad (10)$$

3.3.2 Heat Balance Equations

Heat Balance of Feed Water Heaters

A lower temperature than that of natural environment cannot be utilized, therefore, the large amount of heat rejected from the condenser is wasted. To mitigate such heat waste, regenerative feed water heaters (FWHs) are employed in which feed water is heated to its final temperature by extracted steam from various stages of turbines.

There are two different types of FWHs commonly used in power plants: open FWH, and closed FWHs, where a heat exchanger is used to transfer heat between two streams, which can be maintained at different pressures.

♦ Closed feed water heaters

Most feed water heaters are shell-and-tube heat exchangers, although some are of the header type. A few employ straight tubes, although the majority uses U-tubes, which are relatively tolerant to the thermal expansion during operation.

In shell and tube closed FWHs, the condensed steam, on the shell side, from each feed water heater drains successively to the next lower pressure heater and is returned to the feed water by means of heater drain pumps or through the condenser. The heat balance equation is

$$\dot{m}_{st} * (h_1 - h_2) = \dot{m}_{fw} * (h_{out} - h_{in}) \quad (11)$$

where \dot{m}_{st} = steam mass flow rate extracted from turbine

to feed water heater, kg/s, \dot{m}_{fw} = feed water mass flow rate inlet to feed water heater, kg/s, h_1 = enthalpy of steam inlet to feed water heater, kJ/kg, h_2 = enthalpy of steam outlet from feed water heater, kJ/kg, h_{in} = enthalpy of mixture inlet to feed water heater, kJ/kg, and h_{out} = enthalpy of feed water outlet from feed water heater, kJ/kg.

◆ Deaerator

Dissolved oxygen and carbon dioxide in the feed water fed to the boiler cause internal corrosion of pipes. Thus, it is extremely important to get rid of all dissolved gases from feed water, and this is achieved by using a deaerator, which is an open feed water heater. Equipment life can be extended at little or no cost by limiting the oxygen concentration to 5 ppb. Dissolved CO₂ is essentially completely removed by the deaerator.

Deaerators in steam generating systems of most thermal power plants use low pressure steam obtained from an extraction point in their steam turbine system. The heat balance is

$$(\dot{m}_{st} + \dot{m}_{fw}) * h_{out} = (\dot{m}_{st} * h_1) + (\dot{m}_{fw} * h_{in}) \quad (12)$$

where \dot{m}_{st} = mass flow rate of Steam extracted from turbine to deaerator, kg/s, \dot{m}_{fw} = mass flow rate of Feed water inlet to deaerator, kg/s, h_1 = enthalpy of steam inlet to deaerator, kJ/kg, h_{in} = enthalpy of feed water inlet to deaerator, kJ/kg, and h_{out} = enthalpy of feed water outlet from deaerator, kJ/kg.

Heat Balance of Moisture Separator and Reheater

During expansion through the HP section, the moisture content in the steam increases to approximately 12% at the HP turbine exhaust. Moisture in the steam reduces the mechanical efficiency in the LP turbines and causes erosion of LP turbine blades.

The separator may be separate from the reheater or integral with it. Separate separators usually employ centrifugal principles. In integral ones, sudden changes in the steam direction, by means of vanes or baffles, causing loss in the moisture momentum, thus falls down and get separated from the steam. The heat balance of the separator is

$$\dot{m}_r * (h_1 - h_2) = (\dot{m}_s * h_s) + ((\dot{m}_{st} - \dot{m}_s) * h_{out}) - (\dot{m}_{st} * h_{in}) \quad (13)$$

where \dot{m}_{st} = mass flow rate of steam inlet to moisture separator and reheater, kg/s, \dot{m}_s = mass flow rate of water drained from moisture separator and reheater to deaerator, kg/s, \dot{m}_r = mass flow rate of reheating steam inlet to moisture separator and reheater, kg/s, h_{in} = enthalpy of steam with moisture inlet to moisture separator and reheater, kJ/kg, h_{out} = enthalpy of superheated steam outlet from moisture separator and reheater, kJ/kg, h_s = enthalpy of water drained from moisture separator and reheater to deaerator, kJ/kg, h_1 = enthalpy of reheating steam inlet to moisture sep-

arator and reheater, kJ/kg, and h_2 = enthalpy of reheating steam outlet from moisture separator and reheater to steam generator, or feed water heater, kJ/kg.

Heat Balance of Cooling Water System (condenser)

The rise in cooling water temperature and mass flow rate is related to the heat rejected in the condenser as

$$Q_{Rej} = (\dot{m}_{mix} * h_{in}) - (\dot{m}_{fw} * h_{out}) \quad (14)$$

$$Q_{Rej} = \dot{m}_{CW} * C * \Delta T \quad (15)$$

$$\Delta T = (T_{cwo} - T_{cwi}) \quad (16)$$

$$Q_{Rej} = U * A * LMTD \quad (17)$$

$$LMTD = \left(\frac{(T_{cwo} - T_{cwi})}{\ln \left(\frac{(T_c - T_{cwi})}{(T_c - T_{cwo})} \right)} \right) \quad (18)$$

where \dot{m}_{CW} = cooling water mass flow rate of condenser, kg/s, \dot{m}_{fw} = feed water mass flow rate of outlet from condenser, kg/s, \dot{m}_{mix} = mixture mass flow rate inlet to condenser, kg/s, h_{in} = enthalpy of mixture inlet to condenser, kJ/kg, h_{out} = enthalpy of feed water outlet from condenser, kJ/kg, T_c = Condenser saturation temperature, °C, T_{cwo} = temperature of cooling water outlet from condenser, °C, T_{cwi} = temperature of cooling water inlet to condenser, °C, ΔT = temperature different between the cooling water exit and inlet temperature, °C, U = Overall heat transfer coefficient, W/m²K, C = specific heat of water, kJ/kgK, A = heat transfer area, m², and LMTD = log mean temperature difference, °C.

3.4 Important Factors Affected by Changes in Cooling Seawater Temperature, Fouling Factor, and Salinity

◆ Inside overall heat transfer coefficient, U_i is

$$U_i = \frac{1}{(A_i * (R_i + R_w + R_o + R_{f,i} + R_{f,o}))} \text{ W/m}^2\text{K} \quad (19)$$

where A_i = inside tube surface area, m², R_i = thermal resistance of inner seawater, K/W, R_o = thermal resistance of outer condensation film, K/W, R_w = thermal resistance of tube wall, K/W, $R_{f,i}$ = fouling factor thermal resistance inside condenser tubes, K/W, and $R_{f,o}$ = fouling factor thermal resistance outside condenser tubes, K/W.

◆ Outside overall heat transfer coefficient, U_o is

$$U_o = \frac{1}{(A_o * (R_i + R_w + R_o + R_{f,i} + R_{f,o}))} \text{ W/m}^2\text{K} \quad (20)$$

where A_o = outside tube surface area, m², R_i = thermal resistance of inner seawater, K/W, R_o = thermal resistance of outer condensation film, K/W, and R_w = thermal resistance of tube wall, K/W, $R_{f,i}$ = fouling factor thermal resistance inside condenser tubes, K/W, and $R_{f,o}$ = fouling factor thermal resistance outside condenser tubes, K/W.

◆ Thermal resistance of inner seawater, R_i is

$$R_i = \frac{1}{A_i \cdot h_i} \text{ K/W} \quad (21)$$

where A_i = inside tube surface area, m^2 , and h_i =heat transfer coefficient for flow inside circular tubes, $W/m^2 \text{ K}$.

◆ Thermal resistance of outer seawater, R_o is

$$R_o = \frac{1}{A_o \cdot h_o} \text{ K/W} \quad (22)$$

where A_o = outside tube surface area, m^2 , and h_o = film condensation heat transfer coefficient in bundles of horizontal tubes, $W/m^2 \text{ K}$.

◆ Thermal resistance of tube wall, R_w is

$$R_w = \frac{\ln\left(\frac{r_o}{r_i}\right)}{2 \pi L k} \text{ K/W} \quad (23)$$

where k = thermal conductivity of tube, $W/m \text{ K}$, r_o = outer radius, m , r_i = inner radius, m , and L = tube length, m .

◆ Thermal resistance of seawater fouling factor, R_f is

$$R_f = \frac{F}{A} \text{ K/W} \quad (24)$$

where A = tube surface area, m^2 , and F = fouling factor, $m^2 \text{ K/W}$.

◆ Heat transfer coefficient of flow inside circular tubes, h_i

$$h_i = \frac{Nu \cdot k_{sw}}{d} \text{ W/m}^2 \text{ K} \quad (25)$$

where:

$$Nu_u = 0.023 \cdot R_e^{0.8} \cdot P_r^{0.4} \quad (26)$$

$$R_e = \frac{\rho_{sw} \cdot V \cdot d}{\mu_{sw}} \quad (27)$$

$$P_r = \frac{\mu_{sw} \cdot C_{p,sw}}{k_{sw}} \quad (28)$$

where ρ_{sw} = seawater density, kg/m^3 , V = flow velocity, m/s , d = tube diameter, m , μ_{sw} = seawater dynamic viscosity, $N/m^2 \cdot s$, k_{sw} = seawater thermal conductivity, $W/m \text{ K}$, and $C_{p,sw}$ = seawater specific heat capacity, $J/kg \text{ K}$.

◆ Film condensation heat transfer coefficient in bundles of horizontal tubes, h_o is [25]

$$h_o = 0.725 \left(\frac{g \cdot \rho_l \cdot (\rho_l - \rho_v) \cdot h_{fg} \cdot k^3}{\mu_l \cdot (T_{st} - T_w) \cdot N_h \cdot d_o} \right)^{0.25} \text{ W/m}^2 \text{ K} \quad (29)$$

where ρ_l = liquid density, kg/m^3 , ρ_v = Steam or vapor density, kg/m^3 , μ_l = liquid dynamic viscosity, $N/m^2 \cdot s$, T_{st} = steam or vapor saturation temperature, $^{\circ}C$. N_h = number of horizontal tubes, h_{fg} = latent heat for condensation, kJ/kg , k = thermal conductivity of liquid, $W/m \text{ K}$, g = acceleration of gravity, m/s^2 , and T_w = condenser tube surface wall temperature, $^{\circ}C$.

◆ Seawater density, ρ_{sw}

The density of seawater, ρ_{sw} as a function of temperature, pressure, and salinity is a fundamental oceanographic property. The thermo-physical seawater density correlation is given as [26]

$$\rho_{sw} = \left(\frac{(a_1 + a_2 T + a_3 T^2 + a_4 T^3 + a_5 T^4) + (b_1 S_p + b_2 S_p T + b_3 S_p T^2 + b_4 S_p T^3 + b_5 S_p T^4)}{1} \right) \text{ kg/m}^3 \quad (30)$$

where:

$$a_1 = 9.999 \times 10^2, \quad a_2 = 2.034 \times 10^{-2}, \quad a_3 = -6.162 \times 10^{-3}, \quad a_4 = 2.261 \times 10^{-5}, \quad a_5 = -4.657 \times 10^{-8},$$

$$b_1 = 8.020 \times 10^2, \quad b_2 = -2.001, \quad b_3 = 1.677 \times 10^{-2}, \quad b_4 = -3.060 \times 10^{-5}, \quad b_5 = -1.613 \times 10^{-5}, \text{ and valid for } \rho_{sw} \text{ in } (kg/m^3) \text{ for } 0 \leq T \leq 180 \text{ }^{\circ}C, \text{ and } 0 \leq S_p \leq 0.16 \text{ kg/kg, with accuracy } \pm 0.1 \text{ \%}.$$

◆ Seawater specific heat, C_{psw}

The specific heat of seawater, C_{psw} changes as a function of both temperature and salinity. The thermo-physical seawater specific heat correlation is [26]

$$C_{psw} = A + B T + C T^2 + D T^3 \text{ kJ/kg K} \quad (31)$$

where:

$$A = 5.328 - 9.76 \times 10^{-2} S_p + 4.04 \times 10^{-4} S_p^2,$$

$$B = -6.913 \times 10^{-3} + 7.351 \times 10^{-4} S_p - 3.15 \times 10^{-6} S_p^2,$$

$$C = 9.6 \times 10^{-6} - 1.927 \times 10^{-6} S_p + 8.23 \times 10^{-9} S_p^2,$$

$$D = 2.5 \times 10^{-9} + 1.666 \times 10^{-9} S_p - 7.125 \times 10^{-12} S_p^2, \text{ and}$$

the validity of C_{psw} in ($kJ/kg \text{ K}$) is for $273.15 < T < 453.15 \text{ K}$, and $0 < S_p < 180 \text{ g/kg}$, with accuracy of $\pm 0.28\%$.

◆ Seawater thermal conductivity, k_{sw}

The thermal conductivity, k_{sw} is an important property of seawater and one of the most difficult liquid properties to measure. Consequently data on seawater thermal conductivity is very limited. For aqueous solutions containing an electrolyte, such as seawater, the thermal conductivity usually decreases with an increase in the concentration of dissolved salts. The thermo-physical seawater thermal conductivity correlation is [26]

$$\log_{10}(k_{sw}) = \log_{10}(240 + 0.0002 S_p) + 0.434 \left(2.3 - \frac{343.5 + 0.037 S_p}{T + 273.15} \right) \left(1 - \frac{T + 273.15}{647 + 0.03 S_p} \right)^{0.333} \text{ W/m K} \quad (32)$$

where the validity is for k_{sw} in $W/m \text{ K}$, is for $0 < T < 180 \text{ }^{\circ}C$ and $0 < S_p < 160 \text{ g/kg}$, with accuracy of $\pm 3\%$.

◆ Seawater dynamic viscosity, μ_{sw}

The dynamic viscosity of seawater, μ_{sw} changes as a function of both temperature and salinity. The thermo-physical seawater dynamic viscosity correlation is [26]

$$\mu_{sw} = \mu_w (1 + A S_p + B S_p^2) \text{ kg/m s} \quad (33)$$

where:

$$A = 1.541 + 1.998 \times 10^{-2} T - 9.52 \times 10^{-5} T^2,$$

$$B = 7.974 - 7.561 \times 10^{-2} T + 4.724 \times 10^{-4} T^2,$$

$$\mu_w = 4.2844 \times 10^{-5} + (0.157 (T + 64.993)^2 - 91.296)^{-1}, \text{ and}$$

the validity is for μ_{sw} and μ_w in ($kg/m \cdot s$) for $0 < T < 180 \text{ }^{\circ}C$ and $0 < S_p < 0.15 \text{ kg/kg}$, with accuracy: $\pm 1.5\%$.

3.5 The Effect of Condenser Performance on the Thermal Performance of the Plant

The present model studies the effect of the condenser efficiency, η_c on the exhaust steam temperature and pressure, condenser loss factor (LF), and output power and thermal efficiency of the power plant. The condenser

loss factor is defined as the ratio of the heat released by the steam entering the condenser to the heat gained by its cooling water. The loss factor, output power and thermal efficiency are related to the condenser efficiency, η_c as [27].

$$\eta_c = \left(\frac{T_{cwo} - T_{cwi}}{T_c - T_{cwi}} \right) \% \quad (34)$$

$$LF = \left(\frac{Q_{Rej, st}}{Q_{Rej, cw}} \right) \quad (35)$$

$$LF = \left(\frac{\dot{m}_{mix} * h_{in} - (\dot{m}_{fw} * h_{out})}{\dot{m}_{cw} * C * \Delta T} \right) \quad (36)$$

where $Q_{Rej, st}$ = heat rejected from condensate steam, kW, $Q_{Rej, cw}$ = heat rejected from condensate steam to cooling water, kW, \dot{m}_{mix} = mass flow rate of mixture inlet to condenser, kg/s, \dot{m}_{fw} = mass flow rate of feed water outlet from condenser, kg/s, \dot{m}_{cw} = mass flow rate of cooling water inlet to condenser, kg/s, h_{in} = enthalpy of mixture inlet to condenser, kJ/kg, and h_{out} = enthalpy of feed water outlet from condenser, kJ/kg.

4. Results and Discussion

4.1 Thermodynamic Data and State Diagrams of Plant Components

Classical thermodynamic heat balance calculations are

performed using computer software engineering equation solver (EES) to determine the thermodynamic properties at inlet and exit of each component in the steam cycle of the assigned BWR NPP. Thus, it will be easy to calculate and quantify all key parameters which indicate the state of the plant such as heat added to steam, heat rejection, turbine output power, and the overall thermal efficiency.

These analyses represent the base to evaluate the impact of climate changes on the thermal performance of the proposed BWR plant. Figure 2 represents the designed heat balance model of the proposed plant at a cooling water temperature of about 5 °C, as obtained from the computer software Probera [28].

Figure 3 illustrates the simplified design heat balance model of the proposed plant at a cooling water temperature of about 5 °C, as created by EES.

Table 2 summarizes the inlet and exit thermodynamic properties for each component in the cycle of the O3 NPP at design conditions.

Figure 4 shows the thermodynamic state of each point and heat balance analysis of the studied plant on the T-s and h-s diagrams of the steam Rankine cycle.

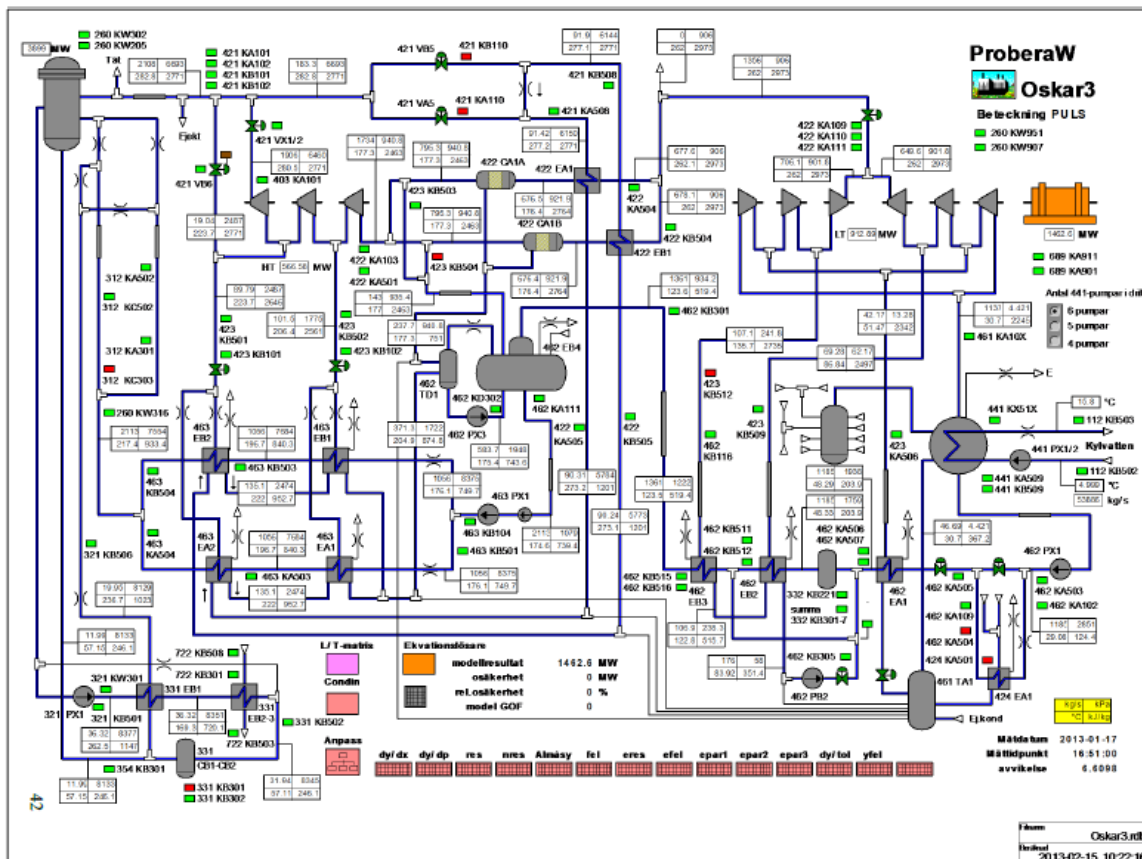


Figure 2. Approximation of the heat balance of the O3 plant at a cooling water temperature of about 5 °C

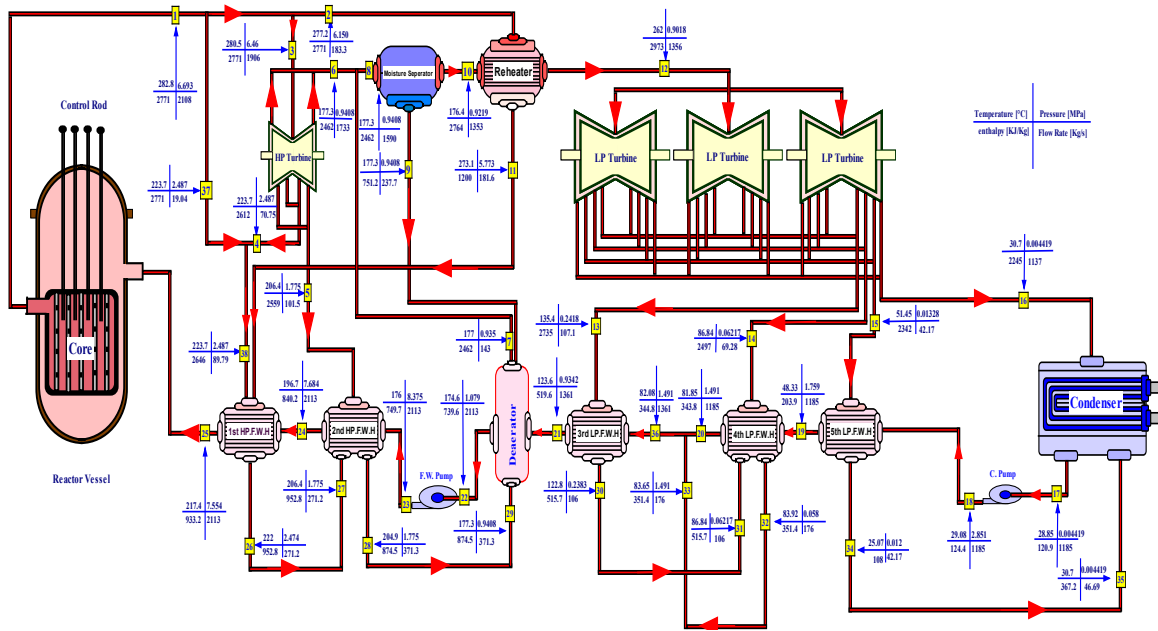


Figure 3. The EES model equivalent of thermodynamic and heat balance analyses for the proposed O3 BWR NPP

Table 2. Thermodynamic data of the plant

Point No.	Temperature, T (°C)	Pressure, p (MPa)	Enthalpy, h (kJ/kg)	Entropy, s (kJ/kg K)	Quality, X	Mass flow rate, (kg/s)
1	282.8	6.693	2771	5.827	0.997	2108
2	277.2	6.15	2771	5.857	0.9929	183.3
3	280.5	6.46	2771	5.8	0.9952	1906
4	223.7	2.487	2612	5.876	0.8968	70.75
5	206.4	1.775	2559	5.888	0.8759	101.5
6	177.3	0.9408	2462	5.912	0.8453	1733
7	177	0.935	2462	5.914	0.8455	143
8	177.3	0.9408	2462	5.912	0.8453	1590
9	177.3	0.9408	751.2	2.113	0	237.7
10	176.4	0.9219	2764	6.592	0.995	1353
11	273.1	5.773	1200	3.004	0	181.6
12	262.5	0.9018	2973	7.028	100	1356
13	135.4	0.2418	2735	7.112	100	107.1
14	86.84	0.06217	2497	7.083	0.9314	69.28
15	51.45	0.01328	2342	7.274	0.8941	42.17
16	30.7	0.004419	2245	7.411	0.8716	1137
17	28.85	0.004419	120.9	0.4206	-100	1185
18	29.08	2.851	124.4	0.4229	-100	1185
19	48.33	1.759	203.9	0.6813	-100	1185
20	81.85	1.491	343.8	1.096	-100	1185
21	123.6	0.9342	519.6	1.566	-100	1361
22	174.6	1.079	739.6	2.087	-100	2113
23	176	8.375	749.7	2.091	-100	2113
24	196.7	7.684	840.2	2.29	-100	2113
25	217.4	7.554	933.2	2.484	-100	2113
26	222	2.474	952.8	2.536	-100	271.2
27	206.4	1.775	952.8	2.54	0.03722	271.2
28	204.9	1.775	874.5	2.377	-100	371.3
29	177.3	0.9408	874.5	2.387	0.06094	371.3
30	122.8	0.2383	515.7	1.558	-100	106
31	86.84	0.06217	515.7	1.578	0.06639	106
32	83.92	0.058	351.4	1.122	-100	176
33	83.65	1.491	351.4	1.117	-100	176
34	25.77	0.012	108	0.3778	-100	42.17
35	30.71	0.004421	367.2	1.231	0.09826	46.96
36	82.08	1.491	344.8	1.099	-100	1361
37	223.7	2.487	2771	6.196	0.9832	19.04
38	223.7	2.487	2646	5.944	0.9152	89.79

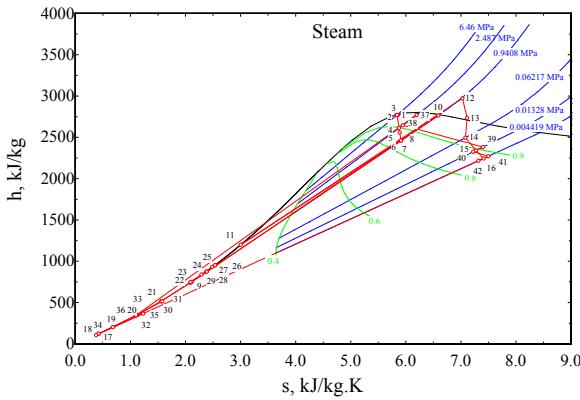
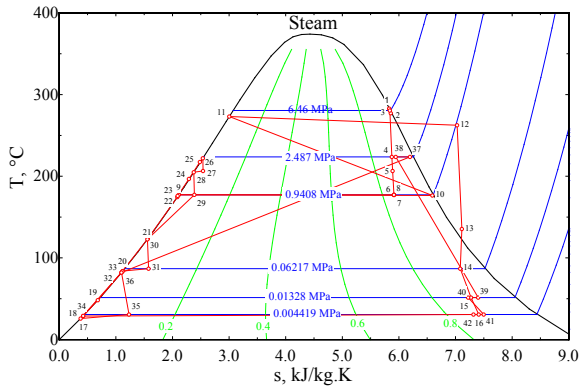


Figure 4. (a) T- s diagram and (b) h- s diagram of the O3 BWR NPP

4.2 The Effect of Condenser Inlet Cooling Water Temperature on \dot{W}_{net} and η_{th}

The results show that as T_{cwi} increases both T_{cwe} and T_C increase. The relation between T_{cwe} and T_{cwi} is found to be linear, since the temperature difference ($T_{cwe} - T_{cwi}$) is constant with nil effect of the condenser terminal temperature difference TTD_c ($T_C - T_{cwe}$). Also, the variation of T_C and T_{cwi} exhibits a linear relationship, with approximately 1 °C difference in T_C for subsequent values of TTD_c at any constant value of T_{cwi} .

Variations of P_c , corresponding to the saturation temperature T_C , with T_{cwi} , resulted in increases in P_c of 0.000259 MPa, 0.000530 MPa, 0.001429 MPa, and 0.003242 MPa, for increases in of 1 °C, 2 °C, 5 °C, and 10 °C, respectively.

When P_c increases, the enthalpy of the extracted steam from low pressure turbines also increases and consequently the output power of turbines decreases. Figure 5 depicts the variation of \dot{W}_{net} with T_{cwi} . It is clearly seen that \dot{W}_{net} decreases as T_{cwi} increases. A decrease in \dot{W}_{net} by 0.4123%, 0.8247%, 2.0618%, and 4.1927% are the result of increases in T_{cwi} of 1 °C, 2 °C, 5 °C, and 10 °C, respectively.

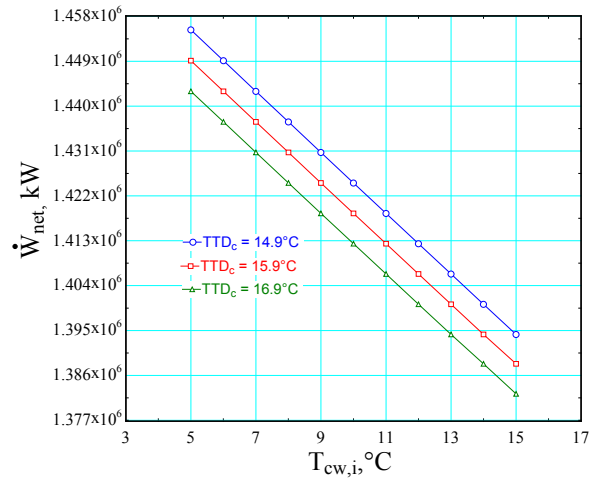


Figure 5. Relation between \dot{W}_{net} and T_{cwi}

Figure 6 presents the variation of η_{th} with T_{cwi} . As shown, η_{th} decreases as T_{cwi} increases. Decreases in η_{th} by 0.16%, 0.32%, 0.8%, and 1.58%, are due to increases in T_{cwi} of 1 °C, 2 °C, 5 °C, and 10 °C, respectively.

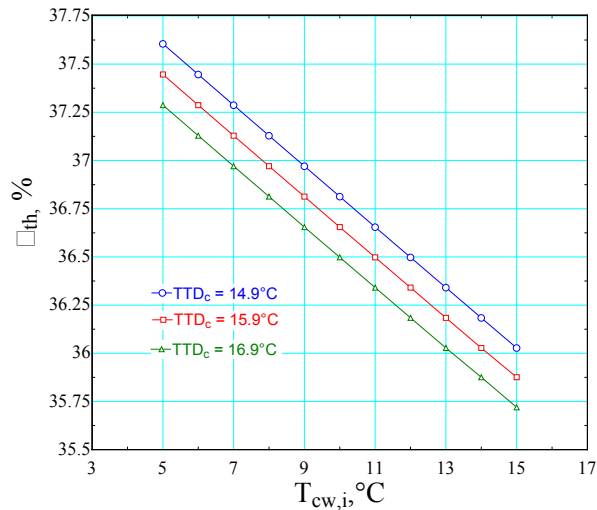


Figure 6. Relation between η_{th} and T_{cwi}

Figure 7 is a summary of the negative impact of variations in T_{cwi} on η_{th} and \dot{W}_{net} of the plant.

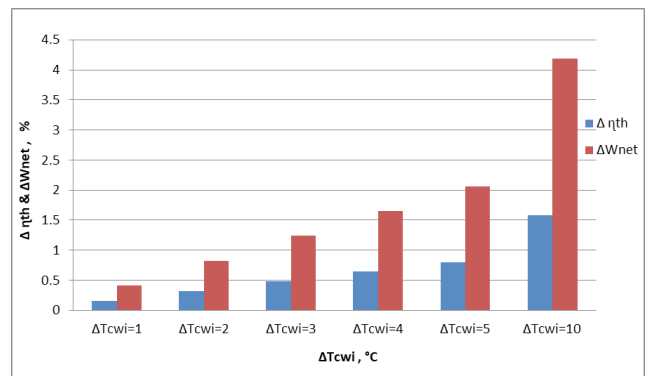


Figure 7. The impact of T_{cwi} on \dot{W}_{net} and η_{th} of the O3 NPP

4.3 The Effect of Condenser Cooling Water Fouling on \dot{W}_{net} and η_{th}

Many factors are affected by changes in T_{cwi} and F_i , such as the inside overall heat transfer coefficient U_i , the outside overall heat transfer coefficient U_o , the condenser temperature T_c , and the condenser vacuum pressure P_c .

It is found that U_i and U_o decrease with increase in F_i and decrease in T_{cwi} . U_i decreases by 24 W/m²K, and 200.4 W/m²K for increases in F_i of 0.00002 m²K/W, and 0.0002 m²K/W, respectively for constant T_{cwi} . U_o decreases by 22.4 W/m²K, and 185.7 W/m²K as F_i increases by 0.00002 m²K/W, and 0.0002 m²K/W, respectively for constant T_{cwi} . These are significant decreases in U_i and U_o .

T_c increased by 0.3 °C and 3 °C for F_i increases of 0.00002 W/m²K, and 0.0002 W/m²K, respectively for constant T_{cwi} . P_c went up to 0.000076 MPa and 0.000816 MPa as F_i increased by 0.00002 m²K/W, and 0.0002 m²K/W, respectively for fixed T_{cwi} .

Figure 8 represents the relation between \dot{W}_{net} and F_i for

different values of T_{cwi} . It is observed that \dot{W}_{net} decreases as F_i and T_{cwi} increase. \dot{W}_{net} decreases by 0.1374% and 1.2371% of the nominal power due to increases in F_i by 0.00002 m²K/W, and 0.0002 m²K/W, respectively for fixed T_{cwi} .

Figure 9 indicates changes in η_{th} with F_i for different values of T_{cwi} . The results show a decrease in η_{th} by 0.05% and 0.48% due to increases in F_i of 0.00002 m²K/W, and 0.0002 m²K/W, respectively at constant T_{cwi} .

Any increase in F_i and T_{cwi} leads to increasing the fouling thermal resistance of the condenser and these lead to a reduction in U_i and U_o . These decreases in the overall heat transfer coefficients cause a decrease in the amount of the heat transferred to the seawater coolant, thus the steam turbine exhaust temperature increases and accordingly the corresponding pressure, which is a power loss.

Figure 10 shows a summary of the effect of F_i on \dot{W}_{net} and η_{th} of the proposed NPP for a constant value of T_{cwi} .

The combined effect of condenser cooling seawater fouling and temperature on, \dot{W}_{net} and η_{th} of the O3 plant are exhibited in Figure 11.

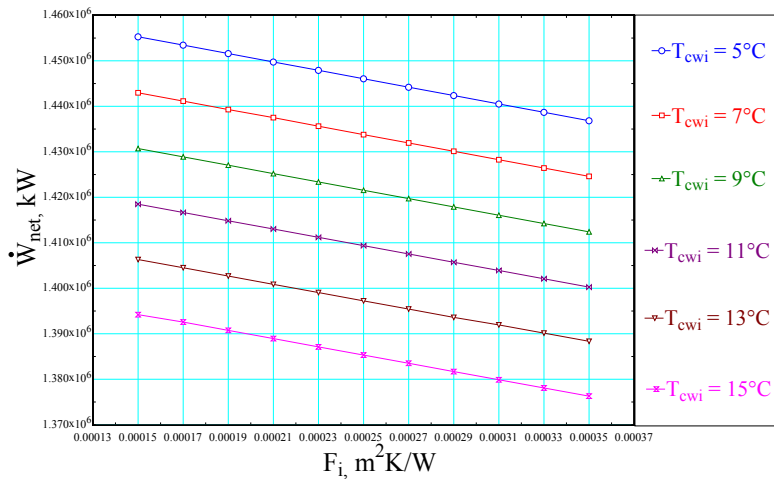


Figure 8. Variations of \dot{W}_{net} with F_i for different values of T_{cwi}

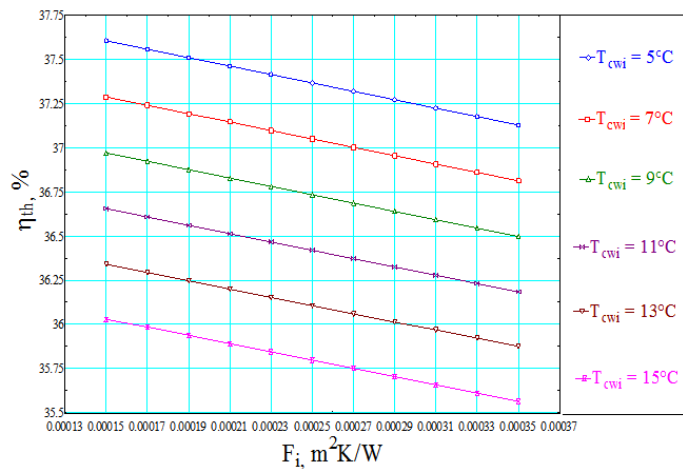


Figure 9. Variation of η_{th} with F_i for different values of T_{cwi}

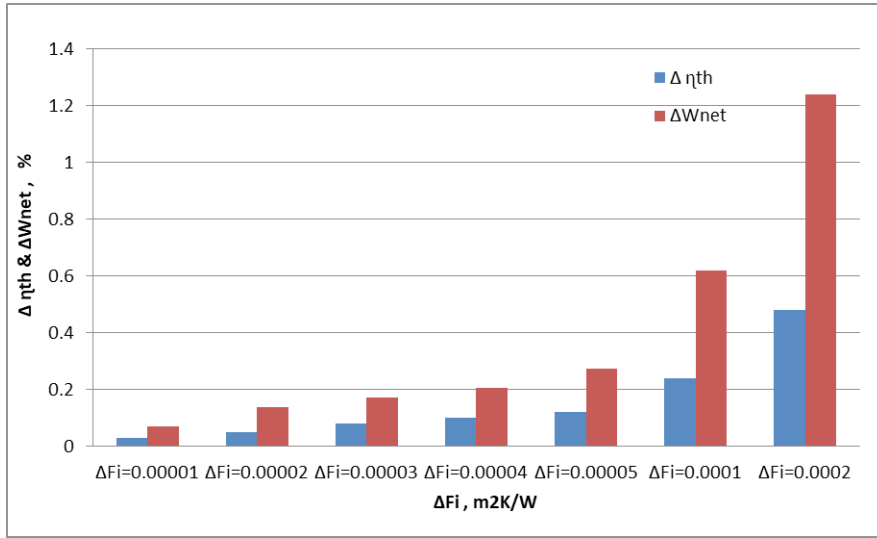


Figure 10. The effect of F_i on the thermal efficiency and output power of the BWR NPP

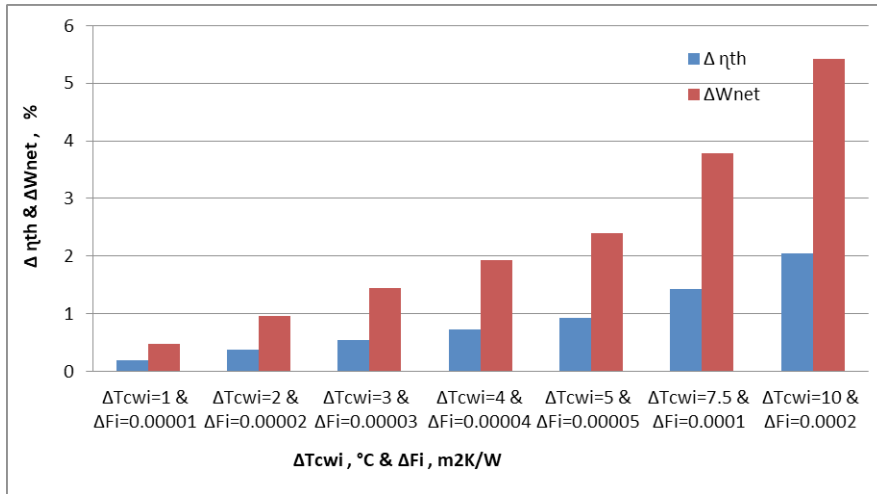


Figure 11. Impact of T_{cwi} and F_i on \dot{W}_{net} and η_{th} of the NPP

4.4 The Effect of Condenser Cooling Water Salinity on \dot{W}_{net} and η_{th}

The model demonstrates that the seawater density ρ_{sw} increases as S_p increases, and decreases with T_{cwi} increase. ρ_{sw} increases by 8 kg/m³ and 79 kg/m³ as S_p increases by 10 g/kg, and 100 g/kg, respectively for constant T_{cwi} .

The results depict that the seawater specific heat, $C_{p,sw}$ decreases with S_p and T_{cwi} increases until the salinity reaches 20%, thereafter the increase in S_p damps out this decrease and the effect of temperature takes over, i.e., $C_{p,sw}$ increases with increasing T_{cwi} . It is depicted that $C_{p,sw}$ decreases by 0.063 kJ/kg.K and 0.525 kJ/kg.K for S_p increases of 10 g/kg, and 100 g/kg, respectively at the same T_{cwi} .

The results give that μ_{sw} increases for S_p increase, and decreases as T_{cwi} increases. μ_{sw} increases by 0.000026 kg/m.s

and 0.000364 kg/m.s for increases in S_p of 10 g/kg, and 100 g/kg, respectively for unchanged T_{cwi} .

The results revealed that the seawater thermal conductivity k_{sw} decreases as S_p increase, and increases with T_{cwi} increase. k_{sw} decreases by 0.0006 W/m.K and 0.0058 W/m.K, as S_p increases by 10 g/kg, and 100 g/kg, respectively at constant T_{cwi} .

Thermal resistance and heat transfer coefficients of the condenser change with changes in all the above mentioned thermo-physical properties of the condenser cooling seawater. The inside tube heat transfer coefficient of the condenser h_i decreases as S_p increases, and increases with increase in T_{cwi} . h_i decreases by 39 W/m²K and 454 W/m²K as S_p increases by 10 g/kg, and 100 g/kg, respectively for fixed T_{cwi} .

The change in h_i results in changing both U_i and U_o . In

fact U_i and U_o decrease as S_p increases, and increase as T_{cwi} increases. U_i and U_o decrease by $2 \text{ W/m}^2\text{K}$ and $1.7 \text{ W/m}^2\text{K}$ for a 10 g/kg increase in S_p , respectively, and by $21 \text{ W/m}^2\text{K}$ and $19.1 \text{ W/m}^2\text{K}$, for S_p increase of 100 g/kg , respectively at constant T_{cwi} .

The decrease in overall heat transfer coefficients of the condenser reduces the output power and thermal efficiency of the plant. Figure 12 shows the relation between \dot{W}_{net} and S_p , at different values of T_{cwi} . It is seen that \dot{W}_{net} decreases as S_p and T_{cwi} increase. \dot{W}_{net} decreases by about 0.0343% and 0.4123% of nominal power, for increases in S_p of 10 g/kg , and 100 g/kg , respectively for a given T_{cwi} .

Figure 13 exhibits the relation between η_{th} and S_p , for some values of T_{cwi} . It is seen that η_{th} decreases approximately by 0.02% and 0.16% , as S_p increases by 10 g/kg , and 100 g/kg , respectively for the same T_{cwi} .

The adverse effects on h_i , which lead to reductions in U_i and U_o are the result of the effects of increased seawater salinity on the thermo physical properties of the condenser coolant. This results in less capability of heat transfer to coolant. Accordingly, the turbine exhaust temperature and pressure increase, which truly reduces \dot{W}_{net} and η_{th} of the plant.

The present results depict that changes in μ_{sw} , due to increases in S_p , produce the worst effect on \dot{W}_{net} and η_{th} of the plant. ρ_{sw} has the least effect on \dot{W}_{net} and η_{th} . The results indicate that an increase in μ_{sw} from 0.001306 kg/m.s to 0.001627 kg/m.s , decreases \dot{W}_{net} by about 2200 kW , and η_{th} by about 0.04% , while an increase in ρ_{sw} from 999.5 kg/m^3 to 1078 kg/m^3 , decreases \dot{W}_{net} by about 500 kW , and η_{th} by nearly 0.0125% .

Figure 14 represents the concluded results of the effect of S_p on \dot{W}_{net} and η_{th} of the selected O3 NPP.

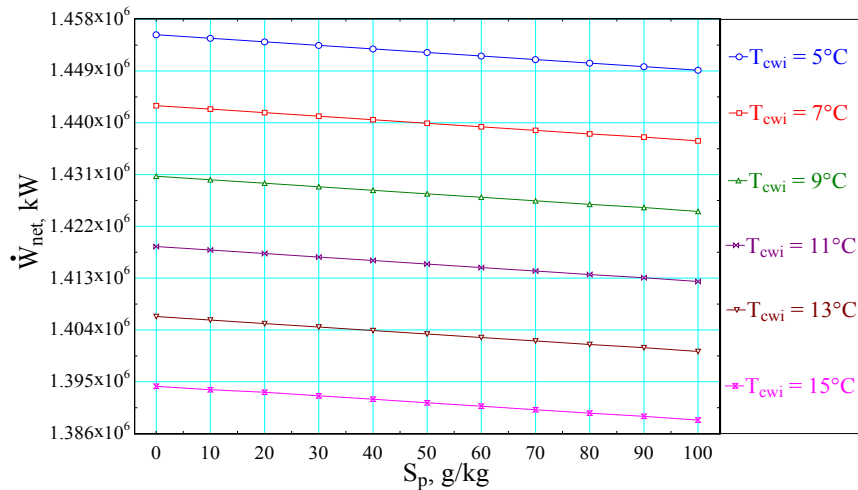


Figure 12. Variations of \dot{W}_{net} , with S_p for different values of T_{cwi}

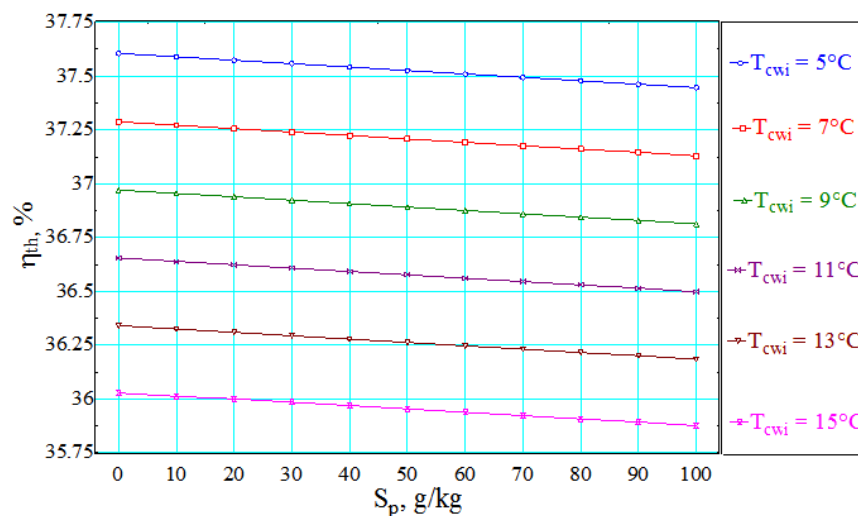


Figure 13. Variations of η_{th} with S_p for different values of T_{cwi}

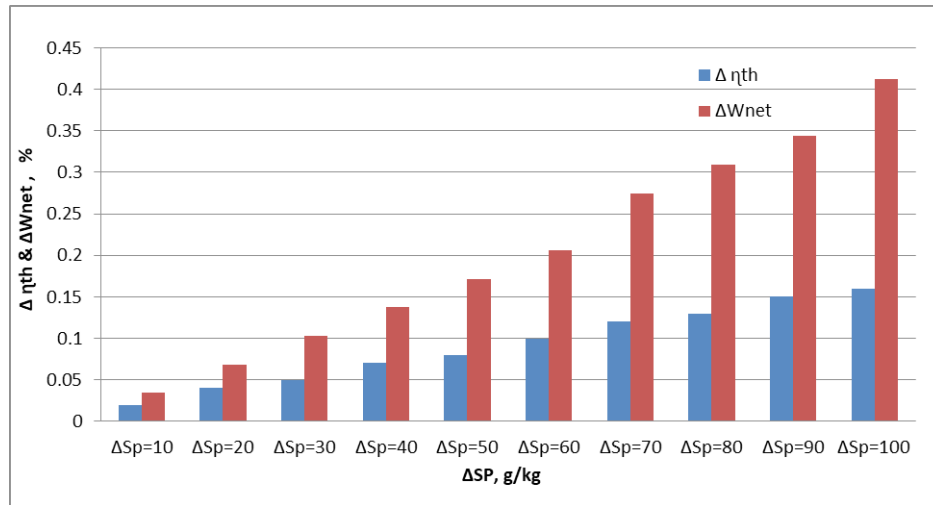


Figure 14. The Effect of S_p on η_{th} and \dot{W}_{net} of the NPP

4.5 The Combined Effect of Condenser Cooling Water Temperature, Fouling Factor, and Salinity on \dot{W}_{net} and η_{th}

The results indicate that U_i and U_o increase with increase in T_{cwi} and decrease with increasing F and S_p , whereas T_c and P_c increase with increasing T_{cwi} , F , and S_p . For 1 °C increase in T_{cwi} , fouling factor of seawater and treated boiler feed water of 0.00002 m²K/W and 0.00001 m²K/W, respectively, and seawater salinity of 10 g/kg, cause decreases in: U_i , and U_o by 34 W/m²K, 30.9 W/m²K, respectively, and increases in T_c , and P_c by 1.44 °C and 0.000377 MPa, respectively. For an increase of T_{cwi} of 10 °C, fouling factor of seawater and treated boiler feed water by 0.0002 m²K/W and 0.0001 m²K/W, respectively, and S_p of 100 g/kg, U_i and U_o are reduced by 261.8 m²K/W and 242 W/m²K, respectively, and T_c and P_c increase by 14.4 °C and 0.004971 MPa, respectively.

The inside and outside overall heat transfer coefficients

increase with temperature increase and decrease as fouling and salinity increase. The combined effect of increasing temperature, fouling, and salinity makes the thermal resistance of the condenser to go up; this explains the observed reductions in U_i and U_o . As a result, the pressure and temperature of the turbine exhaust are raised, which reduce both output power and thermal efficiency of the plant.

Figure 15 presents variations of \dot{W}_{net} with T_{cwi} at different values of fouling factor of seawater F_i , fouling factor of treated boiler feed water F_o , and S_p . It is seen that \dot{W}_{net} decreases by 0.6185% of nominal power when increasing T_{cwi} by 1 °C, F_i and F_o by 0.00002 m²K/W and 0.00001 m²K/W, respectively and S_p by 10 g/kg. For an increase of T_{cwi} by 10 °C, F_i and F_o by 0.0002 m²K/W and 0.0001 m²K/W, respectively, and S_p by 100 g/kg, \dot{W}_{net} decreases by 5.979% of nominal power. These are significant reductions which should be avoided.

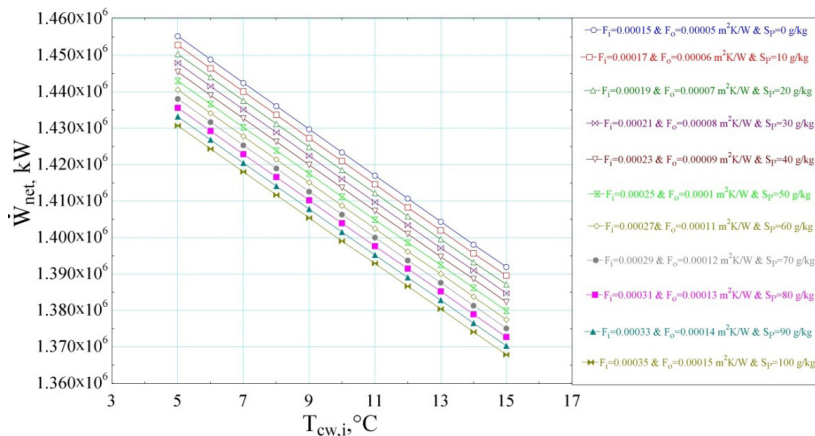


Figure 15. Variations of \dot{W}_{net} T_{cwi} for different values of F_i , F_o and S_p

Figure 16 illustrates variations of η_{th} with T_{cwi} for different values of F_i , F_o , and S_p . As shown η_{th} decreases by 0.23% when increasing T_{cwi} by 1 °C, F_i and F_o by 0.00002 m²K/W and 0.00001 m²K/W, respectively, and S_p by 10 g/kg. For an increase of T_{cwi} by 10 °C, F_i and F_o by 0.0002 m²K/W and 0.0001 m²K/W, respectively, and S_p by 100 g/kg, η_{th} decreases by 2.26%. Such reductions cannot be ignored.

Figure 17 gives the combined impact of T_{cwi} , F_i , F_o , and S_p on both \dot{W}_{net} and η_{th} of the NPP. Quite large losses in \dot{W}_{net} and η_{th} can result from combined variations in condenser cooling sea water temperature, fouling and salinity. It is observed that \dot{W}_{net} and η_{th} of the plant are reduced by 5.979% and 2.26%, respectively for extreme changes in T_{cwi} , F_i , F_o , and S_p .

4.6 The Effect of Condenser Performance on \dot{W}_{net} and η_{th}

Since the condenser is a fundamental player in the thermal efficiency of power plants, therefore, we performed numerical calculations to obtain the effect of changing the condenser efficiency, η_c from 40% - 100 % on the condenser loss factor, LF, exhaust steam pressure, P_c and temperature, T_c , and plant \dot{W}_{net} , and η_{th} .

Figure 18 illustrates the effect of η_c on T_c and P_c . It is seen that T_c and P_c decrease with increasing η_c . For an increase in η_c from 40% - 100%, T_c decreases by about 16.2 °C and P_c decreases approximately by 0.002962 MPa.

The condenser loss factor is reduced as a result of the increase in the amount of heat transferred to the cooling seawater, which is a consequence of the decrease in the

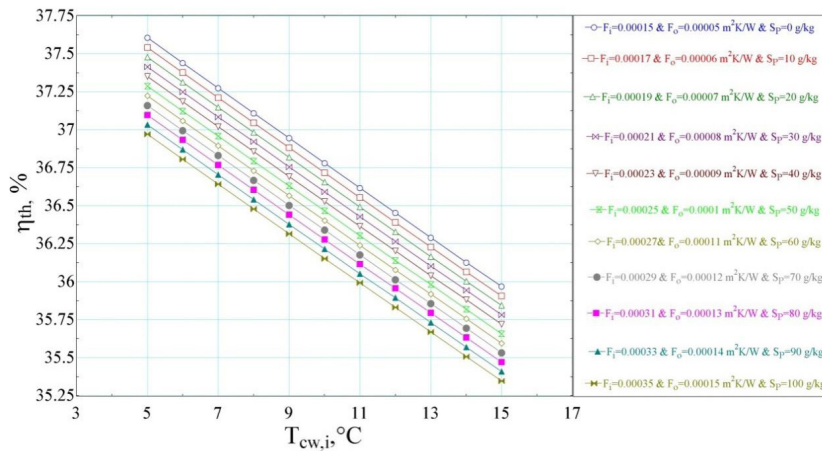


Figure 16. Variations of η_{th} with T_{cwi} at different values of F_i , F_o , and S_p

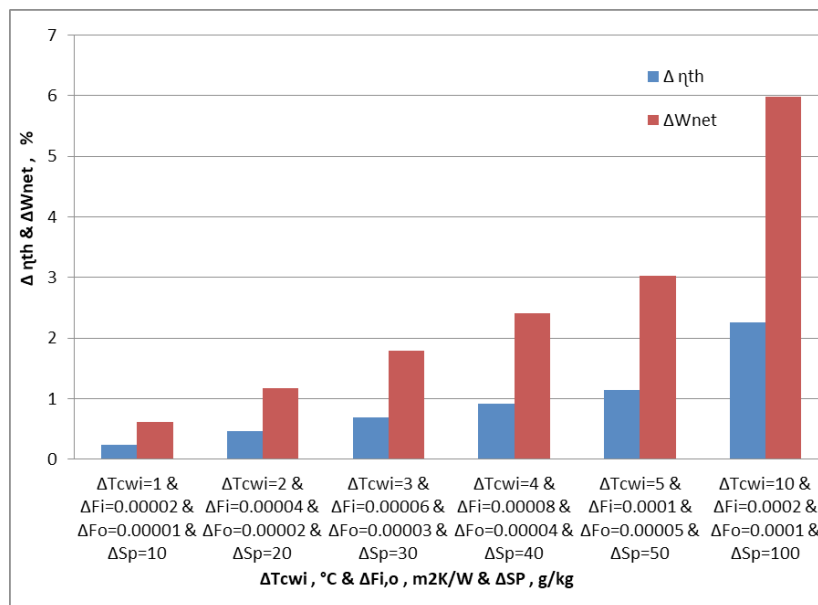


Figure 17. The combined effect of, T_{cwi} , F_i and F_o , and, S_p on \dot{W}_{net} and η_{th}

temperature of the turbine exhaust condensate. Figure 19 presents the effect of η_c , on LF. It is seen that LF decreases with increasing η_c . For an increase in η_c from 40% - 100%, LF decreases by about 0.009.

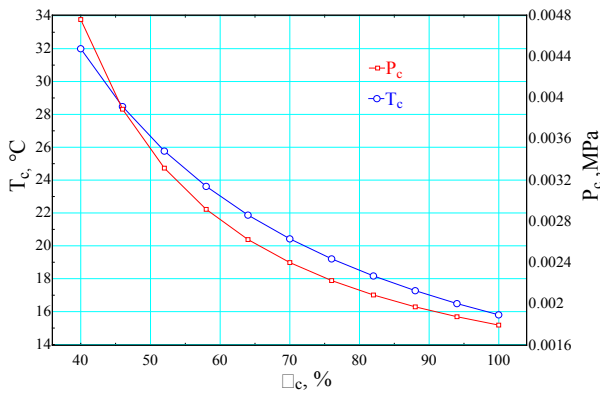


Figure 18. Variations of T_c and P_c , with η_c

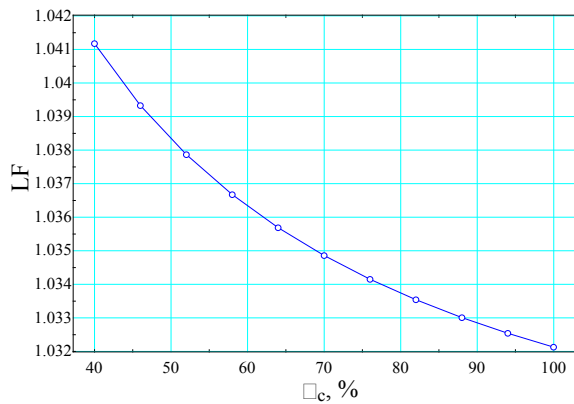


Figure 19. Variations of LF with η_c

The important conclusion is to determine quantitatively the effect of the condenser efficiency, η_c , on \dot{W}_{net} and η_{th} , of the plant. It is clearly shown in Figure 20 that increasing η_c increases both \dot{W}_{net} and η_{th} . For an increase in η_c from 40% - 100%, \dot{W}_{net} increases by 102000 kW, i.e. by 7.049% of the nominal power, and η_{th} increases by 2.62%. These are high adverse effects and should be taken care of.

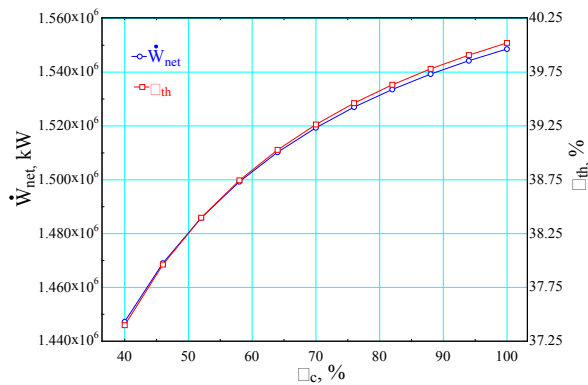


Figure 20. Variations of \dot{W}_{net} and η_{th} with η_c

A decrease in η_c leads to increases in T_c , P_c , and LF. Increases in T_c and P_c translate directly to a power loss and hence less efficient plant. The role of the condenser, as a pivotal component in a power plant, cannot be overlooked. Inefficient condenser can be a burden on the plant. The optimum operating conditions of the condenser must be continuously maintained.

5. Conclusions

The main findings of this research are:

1) An increase of 1 °C in the temperature of the coolant extracted from the sea can result in decreases of 0.4123% and 0.16% in the power output and the thermal efficiency, respectively.

2) The output power and the thermal efficiency are reduced by 1.2371% and 0.48%, respectively for an increase in the fouling factor of the condenser cooling seawater of 0.0002 m²K/W.

3) An increase in the condenser cooling seawater salinity of 100 g/kg, decreases the power output by approximately 0.4123%, and the overall thermal efficiency by about 0.16%.

4) The output power and the overall thermal efficiency are reduced by 5.979% and 2.26%, respectively, for combined extreme increases in the condenser cooling seawater temperature, fouling factor of seawater, fouling factor of treated boiler feed water, and salinity of 10 °C, 0.0002 m²K/W, 0.0001 m²K/W, and 100 g/kg, respectively.

5) A rise in the condenser efficiency from 40% to 100% increases the output power and thermal efficiency by 7.049%, and 2.62%, respectively. Thus, environmental factors and data should be used in the design of these condensers to compensate for the expected decrease in their performance under actual operating conditions during the life time of the NPP. The condenser design and its proper operation are rather important.

The highest adverse impact on the efficiency is due to increases in the condenser seawater cooling temperature, followed by fouling then salinity. Decreases in the thermal efficiency resulting from power losses are significant, and cannot be tolerated. Engineers are working hard and large investments are allocated in order to increase the efficiency by even 0.5% or 1%. The combined negative impacts of all considered factors together are likely to take place rather than their individual effects. Moreover, the extreme values could be achieved in the light, for instance of increased global climate impacts, increasing maritime trade, human activities, and increased water desalination.

The site of NPPs to be built on seas should be carefully selected, in order for changes in characteristics of seawater in the selected site to be a minimum. However,

adverse impacts on the thermal performance of the plant are unavoidable as the operation time goes by, and these should be minimized or eliminated if at all possible. It is recommended to introduce an additional component in new NPPs to keep the seawater condenser coolant temperature, fouling, and salinity within design values. The temperature could be controlled by a heat exchanger working in connection with a refrigeration unit, or/and blow down of hot water and add cold fresh water. Fouling could be controlled chemically, mechanically or otherwise; it is the hardest to deal with. Salinity may be reduced chemically or/and by adding soft water. All could be controlled in one unit with specific sensors for each item, with automatic control operation. The cost of such additional component would be compensated by decreases of the high maintenance costs in NPPs, fuel cost, waste disposal, and keeping the plant operating within its rated efficiency.

The present conclusions should be useful in the design of NPPs in order to avoid the deterioration in the plant's efficiency, which has many adverse technical and economic implications.

Author Contributions

S. Ibrahim: Methodology, Validation, Visualization, Formal analysis, Writing - review & editing, Methodology, Conceptualization, Supervision, Project administration. I. Aggour: Data curation, Software, Methodology, Writing-original draft.

Conflict of Interest

The authors declare that they have no known competing financial interests or personal relationships that could have appeared to influence the work reported in this paper.

Funding

This research did not receive any specific grant from funding agencies in the public, commercial, or not-for-profit sectors.

References

- [1] Ibrahim, S.M.A., Ibrahim, M.M.A., Attia, S.I., 2014. The impact of climate changes on the thermal performance of a proposed pressurized water reactor nuclear-power plant. *International Journal of Nuclear Energy*, Hindawi, Article ID 793908.
- [2] Kim, B.K., Jeong, Y.H., 2013. High cooling water temperature effects on design and operation safety of nuclear power plants in the Gulf region. *Nuclear Engineering and Technology*. 45(7), 961-968.
- [3] Durmaya, A., Sogut, O.S., 2006. Influence of cooling water on the efficiency of a pressurized water reactor nuclear power plant. *International Journal of Energy Research*. 30, 799-810.
- [4] Linnerud, K., Mideksa, T.K., Eskeland, G.S., 2011. The impact of climate change on nuclear power supply. *The Energy Journal*. 32, 149-168.
- [5] Darmawan, N., Yuwono, T., 2019. Effect of increasing seawater temperature on performance of steam turbine of Muara Tawar power plant. *The Journal for Technology and Science*. 30(2), 60-63.
- [6] Pattanayak, L., Padhi, B.N., Kodamasingh, B., 2019. Thermal performance assessment of steam surface condenser. *Case Studies in Thermal Engineering*. 14.
- [7] Prada, S.S., Manichandra, M.G., et al., 2018. Experimental study on performance of steam condenser in 600 MW Singareni thermal power plant. *International Journal of Mechanical Engineering and Technology (IJMET)*. 9(3), 1095-1106.
- [8] Alus, M., Elrawenu, M., Kawan, F., 2017. The effect of the condenser inlet water Temperature on the combined cycle power plant performance. *World Wide Journal of Multidisciplinary Research and Development*. 3(10), 206-211.
- [9] Khan, A.H., Islam, Md.S., 2019. Prediction of thermal efficiency loss in nuclear power Plants due to weather conditions in tropical region. *Energy Procedia*. 160, 84-91.
- [10] Ibrahim, S.M.A., Attia, S.I., 2015. The influence of condenser cooling seawater fouling on the thermal performance of a nuclear power plant. *Progress in Nuclear Energy*. 76, 421-430.
- [11] Alabrudzinski, S., Markuwski, M., Trafczynski, M., et al., 2016. The influence of fouling build-up in condenser tubes on power generated by a condensing turbine. *Chemical Engineering Transactions*. 52, 1225-1230.
- [12] Qureshi, B.A., Zubair, S.M., 2005. The impact of fouling on performance evaluation of evaporative coolers and condensers. *International Journal Energy Research*. 29(14), 1313-1330.
- [13] Muller-Steinhagen, H., 1999. Cooling water fouling in heat exchangers. *Advances in Heat Transfer*. 11, 415-496.
- [14] Bott, T.R., 1995. The design, installation, commissioning and operation of heat exchangers to minimize fouling. *Fouling of Heat Exchangers*, Chapter 13, *Chemical Engineering Monographs*. 26, 269-286.
- [15] Gautam, R.K., Parar, N.S., Vyas, B.G., 2017. Effect of fouling on thermal hydraulic Parameter of shell and tube heat exchanger. Student Conference, Czech Technical University, Prague, Czech Republic.

[16] Ur-Rehman, K.J., Qureshi, B.A., Zubair, S.M., 1994. A comprehensive design and Performance evaluation study of counter flow wet cooling towers. *International Journal of Refrigeration*. 27, 914-923.

[17] Satpathy, K.K., Mohanty, A.K., Sahu, G., et al., 2010. Biofouling and its control in seawater cooled power plant cooling water system - A review. *Nuclear Power*. Pavel Tsvetkov (Ed.).

[18] Ibrahim, S.M.A., Attia, S.I., 2015. The influence of the condenser cooling seawater salinity changes on the thermal performance of a nuclear power plant. *Progress in Nuclear Energy*. 79, 115-126.

[19] Wiesenburg, D.A., Brenda, J.L., 1989. A synopsis of the chemical/physical properties of Seawater. *Ocean Physics and Engineering*. 12(3&4), 127-165.

[20] Ibrahim, M.M.A., Badawy, M.R., 2014. A parametric study of the impact of the cooling water site specific conditions on the efficiency of a pressurized water nuclear power plant. *International Journal of Nuclear Energy*. Article ID 569658.

[21] Sharqawy, M.H., Hussin, I.S., Zubair, S.M., et al., 2011. Thermal evaluation of seawater cooling tower. *Proc. of the ASME 2011 Int. Mechanical Engineering Congress and Exposition*. pp. 1-8. Denver, Colorado.

[22] Taku, N., Jiao, I., et al., 2014. Effects of salinity on heat transfer coefficient of forced convective single phase seawater flow. *Int. Workshop on Nuclear Safety and Sever Accident (NUSSA)*, Kashimo, Japan.

[23] Ibrahim, S.M.A., Attia, S.I., 2015. The combined effect of changes in the condenser cooling seawater temperature, fouling and salinity on the thermal performance of pressurized water reactor nuclear power plant. *International Journal of Nuclear Energy Science & Technology*. 9(1).

[24] Kronblad, R., 2013. *Oskarshamn 3 - optimization after power update*. Lund University.

[25] Holman, J.P., 2010. *Heat Transfer*. 10th Edition. McGraw-Hill.

[26] Sharqawy, M.H., Lienhard, V.J.H., Zubair, S.M., 2010. Thermo physical properties of seawater; A review of existing correlations and data. *Desalination and Water Treatment*. 16, 354-380.

[27] Dutta, A., Das, A.K., Chakrabaru, S., 2014. Study on the effect of cooling water temperature rise on loss factor and efficiency of a condenser for a 210 MW thermal power unit. *International Journal of Engineering Technology and Advanced Engineering*. 3(3), 485-489.

[28] Garland, Wm. J., 2014. *The essential CANDU: A textbook on the CANDU nuclear power plant Technology*. Department of Engineering Physics, McMaster University, Canada.

Nomenclature

A	Heat transfer area	m ²
C	Specific heat	kJ/kg K
d	Diameter	m
F	Fouling factor	m ² K/W
g	Acceleration of gravity	m/s ²
L	Length	m
LF	Loss factor	Dimensionless
LMTD	Log mean temperature difference	°C
h	Enthalpy	kJ/kg
k	Thermal Conductivity	W/m K
m	Mass flow rate	kg/s
N	Number	Dimensionless
Nu	Nusselt number	Dimensionless
P	Pressure	bar
Pr	Prandtl number	Dimensionless
Q	Heat	kJ/kg
R	Resistance	m ² K/W
r	Radius	m
Re	Reynolds number	Dimensionless
s	Entropy	kJ/kg K
S _p	Salinity	g/kg
T	Temperature	°C
ΔT	Temperature difference	°C
U	Overall heat transfer coefficient	W/m ² K
V	Flow velocity	m/s
W	Output power	kJ/kg
X	Moisture content	Dimensionless

Greek Letters

η	Efficiency	%
ρ	Density	kg/m ³
μ	Dynamic viscosity	kg/m.s

Subscripts

ad	Added
c	Condenser
cp	Condensate pump
cw	Cooling water
cwi	Cooling water in
cwo	Cooling water out
f	Reheated steam
h	Horizontal
fw	Feed water
fwp	Feed water pump
HPT	High pressure turbine

v	Vapor
w	Tube wall

Abbreviations

BWR	Boiling water reactor
BPV	Bypass valve
FWH	Feed water heater
HP	High pressure
HPFWH	High pressure feed water heater
HPST	High pressure steam turbine
LPFWH	Low pressure feed water heater
LPST	Low pressure steam turbine
NPP	Nuclear power plant